

Conf -920124--6

Invited paper for Proceedings of 1992 SPIE International Laser Conference.

State-to-state Collision Dynamics of Molecular Free Radicals*

R. Glen Macdonald and Kopin Liu
Argonne National Laboratory
Chemistry Division
Argonne, Illinois 60439

ANL/CP--73598

DE92 006990

ABSTRACT

State-to-state collision dynamics of molecular radicals were investigated by the laser-induced fluorescence technique in a pulsed, crossed-beam apparatus. Dramatically different product state distributions were observed for two prototypical radicals, $\text{NCO}(\tilde{X}^2\Pi)$ and $\text{CH}(\tilde{X}^2\Pi)$. Based on a quantum scattering formalism and general considerations of the potential energy surfaces these observations were interpreted as generic features for the inelastic scattering of $^2\Pi$ radicals. The differences observed for NCO and CH are the results of well-known Hund's coupling classification of linear molecules.

1. INTRODUCTION

The vast majority of chemical reactions have at least one of the reactants and/or products as an open-shell atom or radical. Radical reactivity and energy transfer properties also play a central role in the chemistry of combustion and the atmosphere as well as astrophysics. Despite the importance of radical chemistry to these processes, the experimental and theoretical progress in a detail understanding of the collision dynamics of molecular radicals has been slow. The experimental challenge arises from the transient nature of free radicals, while the theoretical challenge arises because several potential energy surfaces (PES) are involved in describing their collision dynamics.

Radicals are characterized by the existence of unpaired electrons. The unpaired electron endows radicals with fine-structure energy levels induced by the additional couplings due to the unquenched electron orbital and/or spin angular momenta. The spectroscopic consequences of these additional electronic degrees of freedom has long been well-understood. Hund's coupling schemes provide a powerful means of classifying the different spectroscopic features of different radicals. During the past few years, we have been engaged in the systematic study of the collision dynamics of radicals. From these studies, some dynamical consequences of the various Hund's coupling schemes have just begun to emerge. In this paper we present a brief account of these investigations, focussing on one particular feature of the collision dynamics of radicals: How do the product state distributions differ for a Hund's case (a) vs a case (b) Π radical for rotationally inelastic processes? and Why?

2. EXPERIMENTAL

The experiments were conducted in a pulsed, crossed-beam apparatus described previously.¹ A cross sectional view of the apparatus is shown in Fig. 1. The NCO radical beam was generated by photolyzing mixtures of C_2N_2 (~4%)/ O_2 (~10%)/ N_2 (~15%)/ H_2 (~70%) with ArF laser light at 193 nm directly in front of a pulsed molecular beam nozzle. The photolytically generated CN radical reacted almost completely with O_2 to produce NCO. The NCO was subsequently cooled both vibronically and rotationally to a temperature of about 2 K in the strong supersonic expansion.

After colliding with He the product state distribution of $\text{NCO}(\tilde{X}^2\Pi_{3/2,1/2,00^10})$ was interrogated by the saturated laser-induced fluorescence (LIF) technique using the $\text{NCO}(00^00)\tilde{X}^2\Sigma\leftrightarrow(00^10)\tilde{X}^2\Pi$ transition near 440 nm.²

The $\text{CH}(\tilde{X}^2\Pi)$ radical beam was produced by 193 nm multiphoton dissociation of mixtures of $\text{CH}_3(\sim 0.5\%)/\text{Xe}(\sim 3\%)$ and $\text{H}_2(\sim 94\%)$ directly in front of the pulsed molecular beam nozzle. After photolysis and the supersonic expansion approximately 93% of the CH radicals were in the lowest $N=1$ rotational level. The collisionally induced product state distribution was again interrogated by the saturated LIF technique using the $\text{CH} A^2\Delta\leftrightarrow^2\Pi$ transition near 430 nm.³

*Work supported by the U.S. Department of Energy, Office of Basic Energy Sciences, Division of Chemical Sciences, under Contract No. W-31-109-ENG-38.

The submitted manuscript has been authored by a contractor of the U. S. Government under contract No. W-31-109-ENG-38. Accordingly, the U. S. Government retains a nonexclusive, royalty-free license to publish or reproduce the published form of this contribution or allow others to do so, for U. S. Government purposes.

MASTER

2B

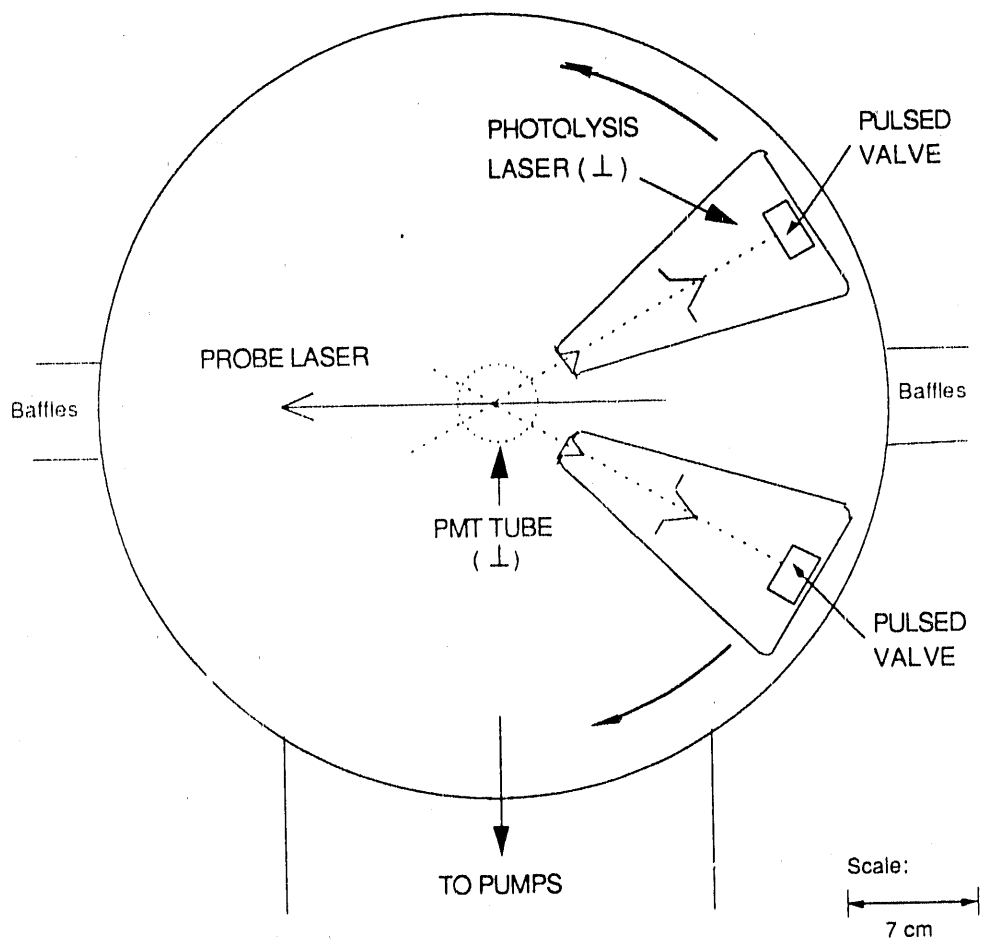
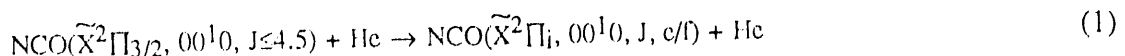


Figure 1. A cross sectional view of the pulsed-molecular beam apparatus. The photomultiplier tube (PMT), recording the LIF, fits in a hollow cylinder in the rotating lid and remains fixed as the beam source rotates. Each pulsed molecular beam source is attached to rotatable lids which cap a cylinder 180 cm long and 60 cm in diameter.

As indicated in Fig. 1, one unique feature of this crossed-beam apparatus is that the state specific detector remains fixed while the two beam sources can be independently rotated; thus, without any change in the expansion conditions, the relative collision energy can be varied merely by changing the intersection angle between the two beams.

3. RESULTS

Figures 2 and 3 show portions of the NCO LIF spectrum for spin-orbit conserving and spin-orbit changing collisions, respectively, at an initial collision energy (E_0) of 3.74 kcal mol⁻¹.⁴ The experiments were conducted by scanning the wavelength of the dye laser while the He beam was alternating on and off. Only the difference spectra, indicating the change in NCO state population induced by collisions with He, are shown. The negative signals for $J \leq 4.5$ in Fig. 2 result from attenuation of the primary NCO beam. The spectra correspond to the inelastic scattering process,



where $i=3/2$ represents spin-orbit conserving transitions, and $i=1/2$ corresponds to spin-orbit changing transitions. For spin-orbit conserving transitions, Fig. 2, the distribution shows a monotonic decline with increasing final J , while for spin-orbit changing collisions, Fig. 3, the distribution is bell-shaped, centered around $J \sim 20.5$. Thus, dramatically different product state distributions for these two types of collision processes are anticipated just from a casual inspection of the LIF spectra.

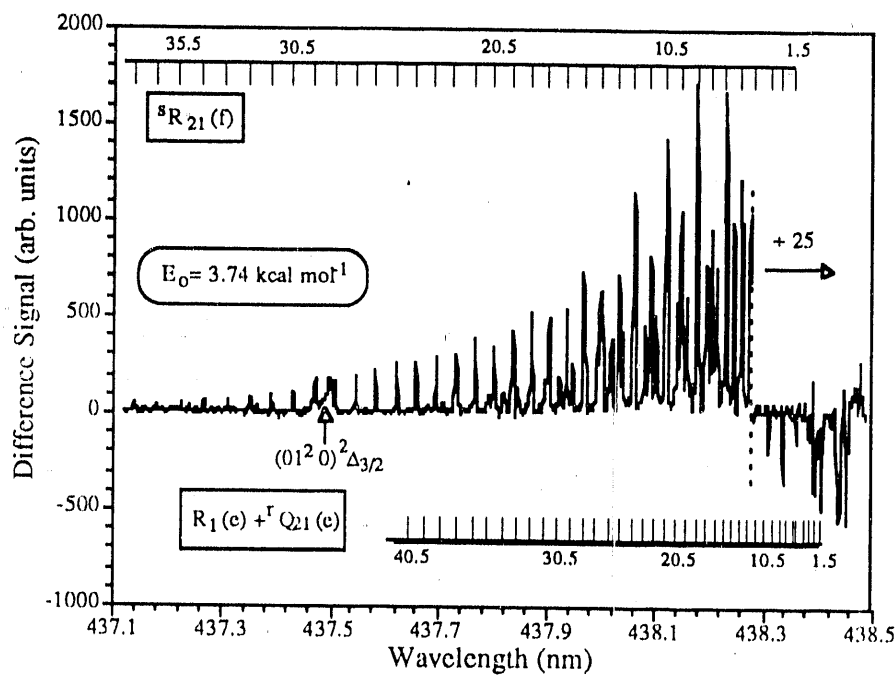


Figure 2. A difference spectrum of the sR_{21} and $R_1 + rQ_{21}$ branches of NCO, corresponding to spin-orbit conserving collisions at an initial translational energy of 3.74 kcal mol⁻¹. The monotonically declining rotational state distribution is clearly evident. The negative going portion of the spectrum to the right of the dotted line results from attenuation of the lowest J states of NCO.

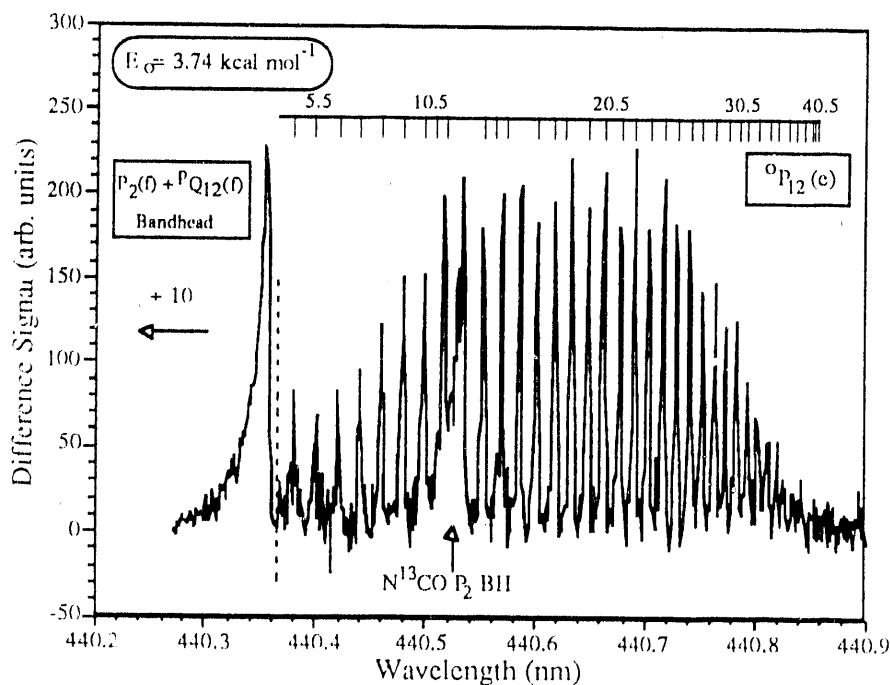


Figure 3. A difference spectrum of the oP_{12} branch of $\text{NCO}({}^2\Pi_{1/2})$ corresponding to spin-orbit changing collisions at a translational energy of 3.74 kcal mol⁻¹. A bell-shaped rotational state distribution is clearly seen.

This anticipation is quantitatively borne out after the complete data analysis. The final rotational state distributions are shown in Fig. 4 for spin-orbit conserving transitions, by the circles, and for spin-orbit changing transitions, by the squares. All the data shown in Fig. 4 have been normalized to one another. It can readily be estimated that the ratio of total cross section for spin-orbit conserving to spin-orbit changing collisions is about 2.2 at $E_0 = 3.74 \text{ kcal mol}^{-1}$. Yet the most remarkable result is that the two processes yield such dramatically different rotational state distributions. In particular, the low J 's population for spin-orbit changing collisions are greatly suppressed. It should be mentioned that the monotonic decline in final rotational population within the $^2\Pi_{3/2}$ manifold is typical for a rotational energy transfer process; however, the bell-shaped distribution in the $^2\Pi_{1/2}$ manifold is quite abnormal.

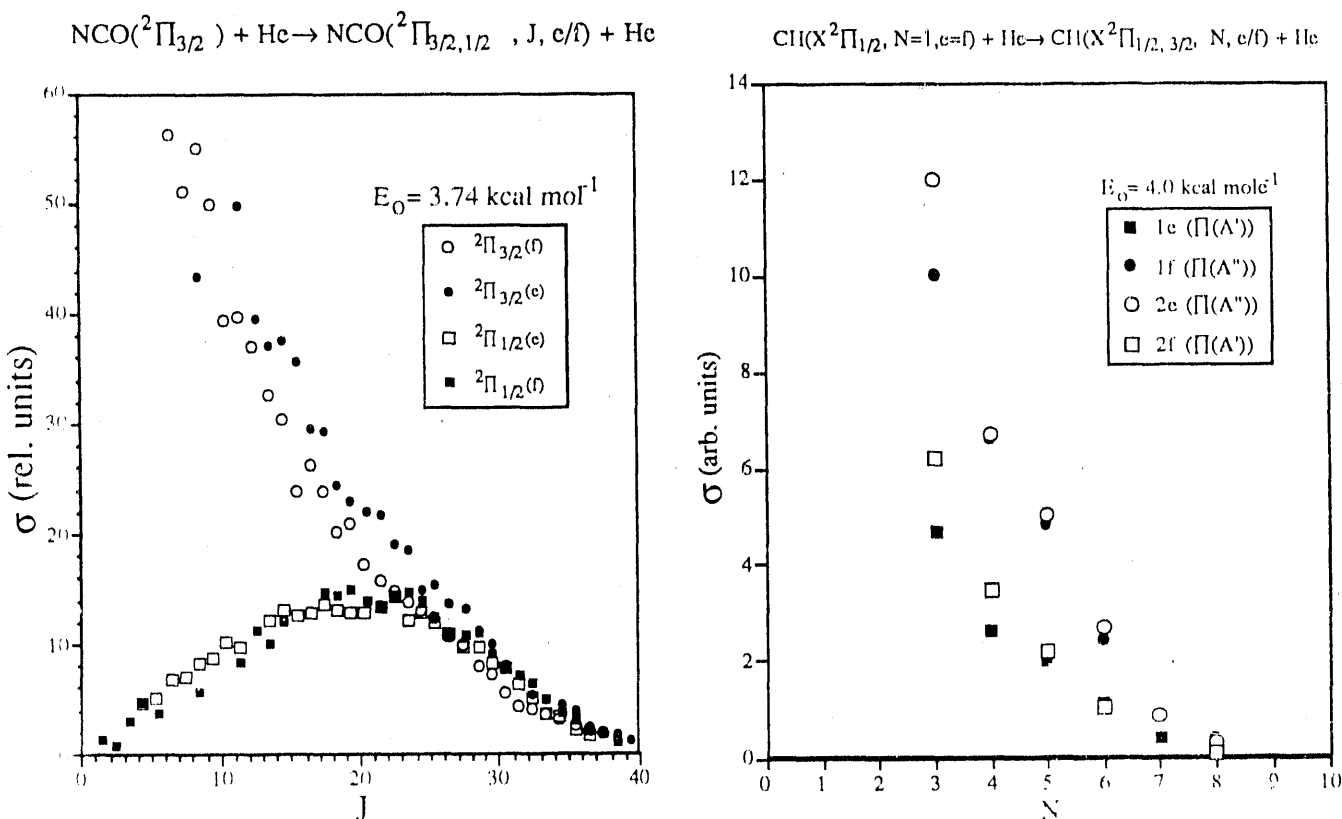


Figure 4. Final rotational state population of $\text{NCO}(\tilde{X}^2\Pi_{3/2,1/2}, 0010)$ from process (1) at a collision energy of $3.74 \text{ kcal mol}^{-1}$.

Figure 5. Final rotational state population of $\text{CH}(\tilde{X}^2\Pi)$ from process (2) at a collision energy of $4.0 \text{ kcal mol}^{-1}$.

Figure 5 shows the results for a similar inelastic scattering process for $\text{CH}(\tilde{X}^2\Pi) + \text{He}$.¹



As can be seen the product state distribution for a given fine-structure manifold always displays a monotonic decline with increasing final N in this case. However, there appears to be two groups of distributions depending on the nature of the fine-structure states. A comparison of Fig. 4 and 5 clearly shows the sharp contrast in the rotational and fine-structure state distributions for $\text{CH} + \text{He}$ compared to $\text{NCO} + \text{He}$.

4. DISCUSSION

To understand the origin of the dramatically different behavior of the product state distributions between process (1) and (2) displayed in Fig. 4 and 5, it should be first realized that the $\text{NCO}(\tilde{X}^2\Pi)$ and $\text{CH}(\tilde{X}^2\Pi)$ radicals are two

prototypical examples of different Hund's cases. The NCO radical has a large spin-orbit constant ($A = -95 \text{ cm}^{-1}$) and a small rotational constant ($B = 0.39 \text{ cm}^{-1}$), i.e. $Y = A/B = -244$; thus, it is an excellent example of an Hund's case (a) radical. On the other hand, the CH radical exhibits nearly perfect Hund's case (b) character (small Y) with $A = 28 \text{ cm}^{-1}$ and $B = 14 \text{ cm}^{-1}$, i.e. $Y = 2$. Physically, these two Hund's cases reflect the competition between the coupling of the electron spin angular momentum with the internuclear axis and that with the nuclear rotational angular momentum.

A typical $^2\Pi$ radical has an electronic configuration with an unpaired electron occupying a p orbital. Depending on the orientation of this unpaired p electron with respect to the collision plane, its interactions with a closed shell (1S) atom are characterized by two non-degenerate PESs of A' (in the plane) or A'' (perpendicular to the plane) in C_s symmetry. These two PESs can be regarded as a pair of Renner-Teller surface because in the collinear approach of the atom with the Π radical the A' and A'' PESs are exactly degenerate. M. Alexander has formulated a rigorous quantum scattering theory for inelastic collisions between a Π radical and a 1S atom.⁵ In this diabatic representation, the collision occurs on neither $V_{A'}$ or $V_{A''}$ PESs, rather the average potential $1/2(V_{A'} + V_{A''})$ and the difference potential $1/2(V_{A''} - V_{A'})$ are used to describe the collision dynamics. From this formal quantum analysis, a number of general propensity rules have been derived and discussed^{5,6} previously and will not be repeated here. Rather, we will outline the underlying physics and applications to the present results.

As usual, the intermolecular interaction is assumed to be purely electrostatic so that a collision can not directly interact with the electron spin of the unpaired electron. A collision can either cause rotational excitation within a given spin-orbit manifold (This interaction is governed by the average potential.) or change both nuclear rotation and the electronic orbital angular momentum motions causing a transition between spin-orbit manifolds and rotational excitation (This interaction is governed by the difference potential.). As shown in Fig. 6, these two different types of collisions represent distinct paths for a Hund's case (a) radical because of the dominance of the spin-orbit interaction. An entirely different situation arises for a Hund's case (b) radical. The strong spin-rotation and weak spin-orbit interaction allows for the decoupling of electron spin from the bond axis. As a result, both the average and difference potentials can contribute to spin-orbit conserving and changing collisions, as depicted in Fig. 6. Furthermore, the existence of two different scattering pathways results in interference of these different scattering amplitudes. One manifestation of this interference is unequal population in the product Λ -doublet states even though initially they were equally populated. For a Hund's case (b) radical Λ -doublet states have well-defined electron orbital alignment with respect to the plane of nuclear rotation; thus, unequal population in Λ -doublet states can be regarded as a preference for orbital alignment from the collision.

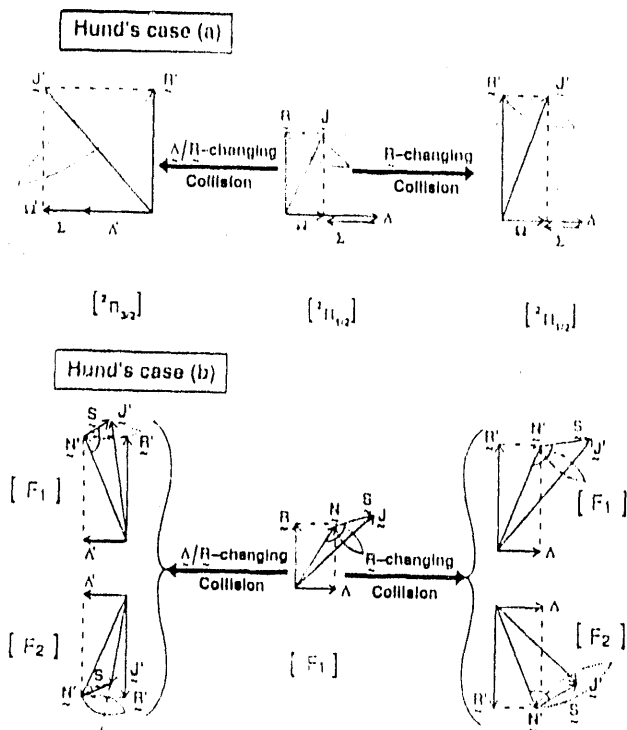


Figure 6. A pictorial representation of angular momenta coupling used to qualitatively visualize the inelastic scattering of a $^2\Pi$ radical and 1S atom.

In general, the interaction of a molecule with a closed-shell atom is expected to be predominantly repulsive with a weak van der Waal's attraction. The presence of unpaired electrons in radicals will result in more anisotropic interactions. However, for the interaction of a $^2\Pi$ radical and a 1S atom either of the adiabatic $V_{A'}$ or $V_{A''}$ PESs are expected to be dramatically different from that expected for closed shell systems. In particular, the average potential is not likely to be very different from that for closed shell systems. For a Hund's case (a) radical such as NCO, as already mentioned, the rotational state distribution for spin-orbit conserving collisions is governed by this average potential and therefore should be similar to those for closed-shell systems, i.e. decline monotonically with increasing ΔJ , as observed in Fig. 4. On the other hand, because $V_{A'}$ and $V_{A''}$ are a pair of mainly repulsive Renner-Teller surfaces, a weak, short-ranged but very anisotropic potential is expected to be the general characteristic of the difference potential. This leads to the reason for the bell-shaped rotational state distribution observed for process (1) as illustrated in Fig. 4. Because the difference potential is short-ranged, only small impact parameter collisions can induce a spin-orbit change. However, large impact parameter collisions are largely responsible for small ΔJ transitions, the very type of collision which experiences only a weak difference potential. Hence the probability of inducing a change in spin-orbit manifold in these types of collisions is small; as a result, small ΔJ transitions are suppressed. Qualitatively, this rationalizes the "missing" population in the low J states for spin-orbit changing, $^2\Pi_{3/2} \rightarrow ^2\Pi_{1/2}$, collisions as seen in Fig. 4.

As mentioned earlier, the simple correspondence for spin-orbit conserving collisions with the average potential and spin-orbit changing collisions with the difference potential is lost for collisions involving a Hund's case (b) radical, for example, process (2). For this case, because the $CH(X^2\Pi)$ radical has an electronic configuration of $^1\pi$, the repulsive interaction will be larger on the $V_{A'}$ surface, where the unpaired p orbital electron lies in the triatomic plane, due to an increase in electron repulsion energy. When the singly occupied p orbital is orientated such that it is perpendicular to the triatomic plane, i.e. the $V_{A''}$ PES, the electron repulsion energy is reduced compared to $V_{A'}$. This results in the difference potential, $1/2(V_{A''} - V_{A'})$ being negative. In the repulsive interaction region, where rotational transitions are largely induced, the average potential is always positive. It has been shown⁶ that this difference in sign between the average and difference potentials leads to constructive interference for Λ -doublet states F_{2e} and F_{1f} labeled by $(\Pi(A''))$ symmetry, in which the unpaired electron is orientated perpendicular to the plane of rotation, and destructive interference for the other two Λ -doublet states F_{2e} and F_{1e} labeled by $(\Pi(A'))$ symmetry in which the unpaired electron lies in the plane of rotation. Accordingly, the preferential production of Λ -doublet states with symmetry $\Pi(A'')$ is expected for equal population in the initial Λ -doublet states. This is exactly what was observed experimentally as shown in Fig. 5.

Because the simple interpretations presented above are based on a quantum scattering formalism and only general considerations of PESs the observed different collisional behavior should be generic features for the inelastic scattering of Hund's case (a) and case (b) radicals with symmetric collision partners. In this regards, similar distributions though not as dramatic as depicted in Fig. 4 have previously been reported for $NO(X^2\Pi, Y = 73)$ with noble gas atoms.⁷ Furthermore, for an intermediate case radical with a $^3\pi$ electronic configuration such as $OH(X^2\Pi, Y = -7.50)$, an opposite Λ -doublet preference to that observed for the CH radical can be predicted from the arguments presented above.⁶ Indeed, this is exactly what has been observed experimentally for $OH + H_2$,⁸ CO and N_2 .⁹

5. SUMMARY and OUTLOOK

In summary, completely different types of collisional behavior have been observed in the inelastic scattering of $^2\Pi$ radicals. We interpreted these observations based on the well known Hund's coupling classification. Extensions of these basic concepts to even more complicated collisional processes such as rovibronic energy transfer and chemical reactions are currently underway. It is hoped that through these systematic investigations a simple classification and better understanding of radical reactivity can eventually be achieved, just as in the case of molecular spectroscopy.

6. ACKNOWLEDGEMENTS

This research was supported by the U.S. Department of Energy, Office of Basic Energy Sciences, Division of Chemical Sciences, under Contract No. W-31-109-ENG-38. Many helpful discussions with A. Wagner are also acknowledged.

7. REFERENCES

1. R.G. Macdonald and K. Liu, "State-to-state integral cross sections for the inelastic scattering of $CH(X^2\Pi) + He$: Rotational rainbow and orbital alignment," *J. Chem. Phys.*, vol. 91, pp. 821-838, July 1989.

2. P.S.H. Boman, J.M. Brown, A. Carrington, I. Koop, and D.A. Ramsay, "A re-investigation of the $A^2\Sigma^+$ - $X^2\Pi_i$ band system of NCO," *Proc. R. Soc. London, Ser A.*, vol. 343, pp. 17- 44, April 1975.

3. I. Bötterud, A. Lofthus and L. Veseth, "Term values and molecular parameters for CH and CH^+ ," *Physica Scripta*, vol. 8, pp. 218-224, 1973.

4. R.G. Macdonald and K. Liu, "Inelastic scattering of NCO($X^2\Pi$) + He: Prototypical rotational state distributions for Hund's case (a) radicals?" *J. Phys. Chem.* vol. 95, pp. 9630-9633, Dec. 1991.

5(a). M.H. Alexander, "Rotationally inelastic collisions between a diatomic molecule in a 2Π electronic state and a structureless target," *J. Chem. Phys.* vol. 76, pp. 5974-5988, June 1982; 5(b) M.H. Alexander, "Quantum treatment of rotationally inelastic collisions involving molecules in Π electronic states: New derivation of the coupling potential," *Chem. Phys.* vol. 92, pp. 337-344, 1985.

6 P. J. Dagdigian, M.H. Alexander, and K. Liu, "The inelastic scattering of 2Π [case (b)] molecules and an understanding of the differing Λ doublet propensities for molecules of π^1 vs π^3 orbital occupancy," *J. Chem. Phys.* vol. 91, pp. 839-848, July 1989.

7. H. Joswig, P. Andresen, and R. Schinke, "Electronic fine structure transitions and rotational excitation in NO rare gas collisions," *J. Chem. Phys.* vol. 85, pp. 1904-1914, August 1986.

8. P. Andresen, N. Aristov, V. Beushausen, D. Hausler, and H.W. Lulf, " Λ -doublet substate specific investigation of rotational and fine structure transitions in collisions of OH with H_2 and D_2 ," *J. Chem. Phys.* vol. 95, pp. 5763-5774, October 1991.

9. D.M. Sonnenfroh, R.G. Macdonald and K.Liu, "A crossed-beam study of the state-resolved integral cross sections for the inelastic scattering of OH($X^2\Pi$) with CO and N_2 ," *J. Chem. Phys.* vol. 94, pp. 6508-6518, May 1991.

END

**DATE
FILMED**

3/3/92

